Vu *et al.*
Journal of Analytical Science and Technology (2024) 15:45
https://doi.org/10.1186/s40543-024-00457-x

Journal of Analytical Science and Technology

SHORT REPORT

Open Access

Exploring the feasibility of a single-protoplast proteomic analysis

Hung M. Vu[1†], Ju Yeon Lee[2,6†], Yongmin Kim[1], Sanghoon Park[1], Fabiana Izaguirre[3], Juhyeon Lee[1], Jung-Hyun Lee[1], Minjoung Jo[3], Hye Ryun Woo[1], Jin Young Kim[2,6*], Pyung Ok Lim[1*] and Min-Sik Kim[1,4,5*]

Abstract

Background Recent advances in high-resolution mass spectrometry have now enabled the study of proteomes at the single-cell level, offering the potential to unveil novel aspects of cellular processes. Remarkably, there has been no prior attempt to investigate single-plant cell proteomes. In this study, we aimed to explore the feasibility of conducting a proteomic analysis on individual protoplasts.

Findings As a result, our analysis identified 978 proteins from the 180 protoplasts, aligning with well-known biological processes in plant leaves, such as photosynthetic electron transport in photosystem II. Employing the SCP package in the SCoPE2 workflow revealed a notable batch effect and extensive missing values in the data. Following correction, we observed the heterogeneity in single-protoplast proteome expression. Comparing the results of single-protoplast proteomics with those of bulk leaf proteomics, we noted that only a small fraction of bulk data was detected in the single-protoplast proteomics data, highlighting a technical limitation of the current single-cell proteomics method.

Conclusions In summary, we demonstrated the feasibility of conducting a single-protoplast proteomic experiment, revealing heterogeneity in plant cellular proteome expression. This underscores the importance of analyzing a substantial number of plant cells to discern statistically significant changes in plant cell proteomes upon perturbation such as abscisic acid treatment in future studies. We anticipate that our study will contribute to advancing single-protoplast proteomics in the near future.

Keywords LC–MS, Single-cell proteomics, Protoplast, Plant, ABA

[†]Hung M. Vu and Ju Yeon Lee have contributed equally to this work.

*Correspondence:
Jin Young Kim
jinyoung@kbsi.re.kr
Pyung Ok Lim
polim@dgist.ac.kr
Min-Sik Kim
mkim@dgist.ac.kr
[1] Department of New Biology, DGIST, Daegu 42988, Republic of Korea
[2] Digital Omics Research Center, Korea Basic Science Institute, Ochang 28119, Republic of Korea
[3] Cellenion SASU, 60 Avenue Rockefeller, Bioserra 2, 69008 Lyon, France
[4] New Biology Research Center, DGIST, Daegu 42988, Republic of Korea
[5] Center for Cell Fate Reprogramming and Control, DGIST, Daegu 42988, Republic of Korea
[6] Critical Diseases Diagnostics Convergence Research Center, Korea Research Institute of Bioscience and Biotechnology, Daejeon 34141, Republic of Korea

Introduction

A leaf, as a photosynthetic organ, plays an important role in the growth and development of plants throughout their entire life as well as responses to the changing environment (Woo et al. 2019). Plant leaves are composed of diverse cell types with different functions. The interplay among diverse leaf cells is essential and should be coordinated to function elaborately in leaves. Investigating how different leaf cell types are spatiotemporally organized and how such an interplay contributes to proper function in physiological and biochemical contexts is desirable to resolve the biological complexity of multi-cellular organs including leaves.

High-throughput sequencing of DNA and RNA in individual cells has revealed that molecular heterogeneity at the single-cell level is greater than previously realized and made important contributions to a comprehensive and holistic understanding of biological processes. However, given that proteins are the primary functional molecules of the cell, and RNA abundances do not directly translate to protein abundances within cells, it is more desirable to identify the proteome at single-cell resolution and to fully understand functional heterogeneity. Furthermore, proteins contain post-translational modifications that are not captured by transcriptomics. Despite its importance, a single-cell proteomic technology is rather limited by several hurdles that must be overcome to comprehensively detect and quantitatively measure the thousands of different proteins in a cell. One of the big hurdles is that proteins, unlike DNA or RNA, cannot be amplified.

Two major technical innovations are required for a successful single-cell proteomics analysis: improved sensitivity of mass spectrometry and reduced sample loss during preparation. Ultra-sensitive mass spectrometers such as timsTOF SCP or Orbitrap Astral have now allowed a proteome analysis at the single-cell level (Lee et al. 2023). Different workflows and methods have been developed for single-cell proteome sample preparation and data analysis, including SCoPE-MS, nanoPOTs, autoPOTs (Lee et al. 2023; Budnik et al. 2018; Liang et al. 2020; Zhu et al. 2018). These methods share a simple rule of thumb of sub-nanoliter volume handling for successful single-cell proteomics. Recently, a high-throughput picoliter dispensing system named CellenONE was introduced for single-cell proteomic sample preparation (Ctortecka et al. 2023). Despite the innovation in single-cell proteomic analysis in recent years, single-cell proteomics has not been applied to the field of plant research. The major obstacle in single-plant cell analysis is cell isolation which may need sophisticated handling because plant cells are covered with cell walls that protect plant cells against mechanical and osmotic stress. In addition, protoplasts are prone to be broken with minute forces, making cell sorting difficult for single-protoplast proteomics (Clark et al. 2022). Recently, a study has attempted to perform single-cell proteomics analysis using *Arabidopsis thalian* root cell types (Montes et al. 2024).

In this study, we explored the limited-scale feasibility of conducting a single-protoplast proteomic analysis derived from leaves by employing a picoliter volume-based sample preparation technique. This analysis enabled us to qualitatively identify 978 proteins from the individual protoplasts. This method was further evaluated by comparing with bulk proteome data acquired from leaves treated with abscisic acid (ABA), one of the stress hormones in plants.

Experimental section

Plant growth conditions, protoplast isolation, and ABA response assay

Arabidopsis thaliana ecotype Columbia-0 (Col-0; wild type) was used in this study. Plants were grown in an experimentally controlled growth room (Korea Instrument, Korea) at 22℃ under 16-h light: 8-h dark photoperiod and photosynthetic photon flux density of 130 μmol m^{-2} s^{-1}. The third and fourth leaves at 12 days after leaf emergence (DAE) were used for the experiment to reduce complexity and variations of results. Protoplasts were isolated as previously described with minor modifications (Kovtun et al. 2000). Briefly, wild-type *Arabidopsis thaliana* (Col-0) rosette leaves were soaked into an enzyme solution (1% cellulase R10, 0.25% macerozyme R10, 0.4 M mannitol, 80 mM $CaCl_2$, and 20 mM MES (pH 5.7) and gently shaken in darkness for 2 h. After shaking, the resulting protoplasts were gently filtered through a miracloth (22–25 μm). The protoplasts were then pelleted at 500 rpm for 5 min (min), washed once with 1 mL of W5 solution (154 mM NaCl, 125 mM $CaCl_2$, 5 mM KCl, 5 mM glucose, and 1.5 mM MES (pH 5.7)), re-pelleted, and resuspended gently in 1 mL of W5 solution. For the ABA response assay, extracted mesophyll protoplasts were placed in 1 mL of W5 solution containing a final concentration of 100 μM ABA or without ABA for 16 h. For bulk leaf proteomic analysis, detached leaves at 12 DAE were floated in the 2-(N-morpholino) ethanesulfonic acid (MES) buffer in the presence or absence of 100 μM ABA.

Single-protoplast proteome sample preparation

Single-protoplast proteome samples were prepared on a CellenONE® instrument as shown in Fig. 1. For the cell lysis and protein digestion, a total 50 nL of a master mix solution containing 0.2% DDM (Sigma), 100 mM TEAB (Sigma), and 10 ng/μL trypsin (Promega) was dispensed into each well before isolation of individual protoplasts. Single-protoplast isolation was achieved under elevated

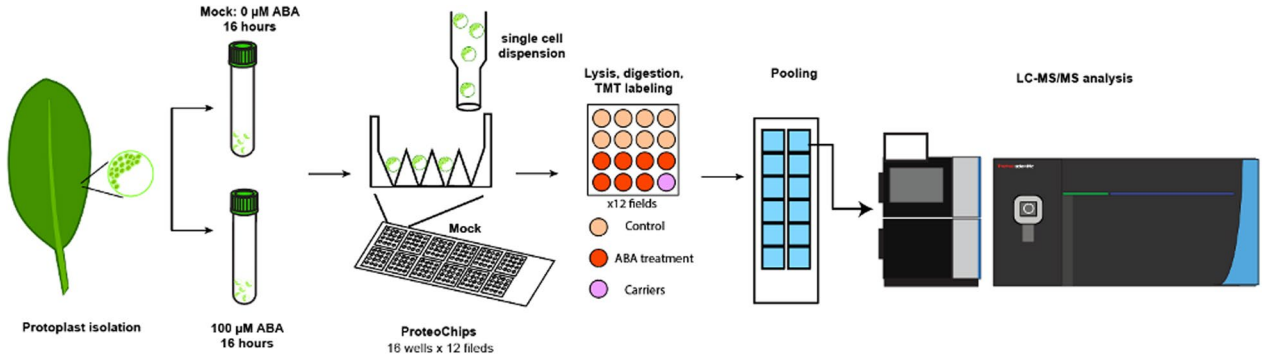

Fig. 1 Experimental workflow of single-protoplast proteomics. Protoplasts isolated from leaves were individually prepared at the single-cell level for a single-protoplast proteomic analysis. For this, proteoCHIP was utilized with nanoliter-volume wells

humidity (85%) to prevent evaporation. Individual cells were sorted into proteoCHIP nanowells with isolation parameters of minimum diameter of 40 µm, maximum diameter of 60 µm, and elongation of 1.4. The mock-treated cells were dispended from well #1 to #8, while ABA-treated cells were dispended from well #9 to #15. For the carrier channel, both ten mock-treated cells and ten ABA-treated cells were dispended to well #16. After single-protoplast isolation, an additional 50 nL of the master mix solution was dispensed to each well. Subsequently, the chip was incubated at 50 °C for 2 h at 80% humidity, directly on the heating deck inside the CelleNONE. For multiplexing, TMTpro™ 16 plex (from 126 to 134 N) dissolved with anhydrous acetonitrile (ACN, Sigma) achieving 5 µg/μL concentration was added to the respective wells (from #1 to #16) and incubated for 30 min at room temperature and 65% humidity. The chemical reaction of the reagents with peptides was quenched with 50 nL of 0.5% hydroxylamine (Thermo) with 1% hydrochloric acid (DAEJUNG). After quenching, 150 nL of 0.1% formic acid was added to adjust final volume to about 3.5 μL, ensuring for subsequent injection into LC–MS. TMT-labeled peptides were pooled via centrifugation (1500×g, 2 min, 25 °C) to the proteoCHIP funnel part and transferred to the autosampler glass vials (SciLab®) for LC–MS/MS. The detailed information about cells and their labeled TMT channel is included in a meta information table (Supplementary Table S1).

Bulk leaf proteome sample preparation

Arabidopsis leaves were ground into fine powder in liquid nitrogen using mortar and pestle. Proteins from leaves were extracted using a lysis buffer containing 5% SDS in 50 mM TEAB. Protein digestion was carried out using an S-trap (ProtiFi) column following the manufacturer protocol. Tryptic peptides were desalted using Sep-Pak C18 1 cc cartridge (Water). Desalted peptides were labeled with TMT reagent, pooled, and fractionated by mid-pH fractionation on an Agilent 1290 Infinity II HPLC system. The mobile phases were composed of 10 mM TEAB in water (A) and 10 mM TEAB in 95% ACN (B). The LC gradient was performed at a flow rate of 0.4 ml/min, started with 5% of B for 5 min, and was linearly ramped to 40% of B for 75 min, and to 90% of B for a minute, and then held at 90% of B for 10 min. Fractionated peptides were combined into 24 fractions and dried for LC–MS.

High-resolution LC–MS for a single-protoplast proteomic analysis

Samples were analyzed using an LC–MS/MS system consisting of an UltiMate 3000 RSLCnano system and an Orbitrap Eclipse Tribrid mass spectrometer (Thermo Fisher Scientific) equipped with a nano-electrospray source. An autosampler was used to load the sample solutions into a C_{18} trap column (Acclaim™ PepMap™ 100, NanoViper, 3 µm particle, 75 µm×2 cm from Thermo Fisher Scientific). The samples were trapped and then desalted and concentrated on the cartridge column for 8 min at a flow rate of 4 µL/min. The trapped samples were then separated on a C_{18} analytical column (PepMap™ RSLC C_{18}, 2 µm, 100 Å, 75 µm×50 cm; Thermo Fisher Scientific). The mobile phases were composed of 100% water (A) and 100% ACN (B), and each contained 0.1% FA. The flow rate was set as 250 nL/min. The LC gradient started with 2% of B for 9 min, and was ramped to 20% of B for 45 min, 32% of B for 15 min and 95% of B for 1 min; it was then held at 95% of B for 10 min and 2% of B for another 1 min. The column was re-equilibrated with 2% of B for 9 min before the next run. A voltage of 1,950 V was applied to produce the gaseous ions. During the chromatographic separation, the Orbitrap Eclipse Tribrid mass spectrometer was operated in data-dependent mode, automatically switching between MS1 and MS2. Full-scan MS1 spectra (375–1200 m/z) were

acquired by the Orbitrap, with a maximum ion injection time of 50 ms at a resolution of 120,000 and normalized automatic gain control (AGC) target set with 250% (2.5×10^6). Top 10 multiply charged precursors (2–5) over a minimum intensity of 5×10^3 were isolated using a 2 Th isolation window. The MS2 spectra were acquired by the Orbitrap mass analyzer at a resolution of 60,000 at a fixed first mass of 110 m/z with HCD (36% normalized collision energy, maximum ion injection time of 118 ms, AGC target value of 5×10^4). Previously isolated precursor ions were subsequently excluded from fragmentation for 120 s within 10 ppm. The internal calibration was conducted with the mass peak set at 445.12003 m/z, which released from polysiloxane from the silica capillary (Keller et al. 2008).

High-resolution LC–MS for a bulk leaf proteomic analysis

Samples were analyzed using an LC–MS/MS system consisting of a Vanquish Neo HPLC (Thermo Fisher Scientific) and a Q Exactive mass spectrometer (Thermo Fisher Scientific) equipped with a nano-electrospray source. An autosampler was used to load the sample solutions into a C_{18} trap column (Acclaim™ PepMap™ 100, NanoViper, 3 µm particle, 75 µm×2 cm from Thermo Fisher Scientific). The trapped samples were then separated on a C_{18} analytical column (PepMap™ RSLC C_{18}, 2 µm, 100 Å, 75 µm×50 cm; Thermo Fisher Scientific). The mobile phases were composed of 100% water (A) and 100% ACN (B), and each contained 0.1% FA. Peptides were separated on a 100-min linear gradient which started from 5% of B, linearly increased to 25% of B at a flow rate of 300 nL/min. The column was finally washed by stabilizing at 90% ACN for 17 min. Precursor ions ranging from 350 to 1650 m/z were acquired at resolution of 70,000 with an automatic gain control (AGC) target of 3×10^6 and maximum injection time of 20 ms. Top 10 abundant ions were selected for fragmentation and acquired at a resolution of 35,000 with an AGC target of 5×10^5 and maximum injection times of 110 ms. The isolation window width was set as 1.4 m/z, and HCD collision energy was set at 27.

Data analysis

Tandem mass spectrometry data were searched against a reference protein sequence database containing 48,359 protein sequences downloaded from the Arabidopsis Information Resource (www.arabidopsis.org) with following searching parameters: acetylation at protein N-termini and oxidation at methionine as variable modifications and up to two missed cleavages by trypsin allowed. False discovery rates were set as 0.01 at both peptide and protein levels.

For single-protoplast proteomics data, the option for isobaric match between run was enabled. The evidence file from MaxQuant searches was further processed using the SCP package (v1.12.0) (Vanderaa and Gatto 2021, 2023). The analysis workflow was done as described in SCoPE2 with minor modifications (Specht et al. 2021). The original PEP values were used without converting to dartPEP. The PSM was controlled at FDR of 1% as in the SCP package workflow. The features with MeanSCR more than 0.8 were filtered out. The cells with a median coefficient of variation (CV) of more than 0.6 were filtered out for further data processing. The cells in two channels (i.e., #14 and #15) next to the carrier channel were considered as impurities and were eliminated prior to downstream analyses. Data were normalized using the median centering method at the protein level. Proteins with more than 30% missing values across all the cells were removed. Missing values were imputed using a K nearest neighbors algorithm, with $k=3$, and batch correction was subsequently performed using ComBat as in the SCoPE2 workflow. Student t test was applied for statistical analysis of both bulk and single-protoplast proteomics data. PCA was done using built-in R function prcomp. UMAP was done using umap package. Gene ontology analysis was performed using PANTHER Classification System (v17.0) (Mi et al. 2013; Thomas et al. 2022).

Results and discussion

Recently, the single-cell proteomics technologies have been successfully developed and applied to studies on animal cells, but there is no report about single-plant cell proteomes. Herein, this study aims to assess if the technique can also be applied to single-plant cells. To do so, we first isolated protoplasts from the third and fourth leaves of Arabidopsis and treated them with or without 100 µM ABA for 16 h.

We then carried a single-cell proteomics analysis by adopting the SCoPE-MS workflow using the recently introduced CellenONE system. Compared to other sample preparation platforms, the workflow on the CellenONE system is known to minimize manual sample handling steps, thus potentially reducing the sample loss and technical variation. Each protoplast was monitored by a camera system to ensure that a cell with a preset cell size was isolated at a time. Single protoplast was dispensed by a nozzle at a 300 picoliter volume to each well of a proteoCHIP which contains multiple nanoliter-volume wells covered with a hexadecane layer as illustrated in Fig. 1. Every mock-treated protoplast was dispensed from wells #1 to #8 of each field, while ABA-treated protoplast from wells #9 to #15. The last well #16 of each field was especially used to pool a total of 20

protoplasts (i.e., 10 mock- and 10 ABA-treated protoplasts). Next, cell lysis, protein digestion, and TMT-based chemical barcoding were performed sequentially on wells for approximately 4 h, during which 70% humidity was maintained to prevent buffer evaporation. Each field of 16 wells containing TMT-barcoded peptide mixtures was pooled together before LC–MS analysis. In summary, a total of 180 protoplasts (i.e., 12 fields × 15 wells) including 96 mock- and 84 ABA-treated protoplasts were analyzed by a high-resolution mass spectrometer.

As a result, a total of 978 proteins were identified by MaxQuant search (Fig. 2A). When performing a gene ontology (GO) analysis using all proteins identified, well-known biological processes (GO:BP), molecular functions (GO:MF), and cellular components (GO:CC) were expected to be found in single-protoplast proteome data. GO:BP showed enrichment of glycogen catabolic process, photosynthetic electron transport in photosystem II, and reductive pentose-phosphate cycle. GO:MF resulted in the enrichment of SHG alpha-glucan phosphorylase activity, linear malto-oligosaccharide phosphorylation activity. Lastly, GO:CC confirmed the subcellular localization in photosystem including I and II complex, chloroplastic endopeptidase Clp complex, or TOC TIC supercomplex I (Table 1). This result indicates that single-protoplast proteomics can be applied to the plant research.

For an in-depth data analysis, we employed the SCoPE2 workflow starting with database searching using MaxQuant followed by data processing with the SCP package (Vanderaa and Gatto 2023, 2021). According to the SCP package, we next examined the median CV of all protoplasts and observed a median CV of around 0.5 for both mock and ABA-treated protoplasts (Fig. 2B). Any protoplast with a median CV of higher than 0.6 was filtered out for further processing, resulting in the number of quantified proteins down to 522 (Fig. 2A). Unexpectedly, all the cells in batch number 10 were filtered out due to a higher median CV. After this, the remained protoplasts were 83 and 52 for mock- and ABA-treated conditions, respectively (Fig. 2A,C).

To find genes altered by ABA at the single-plant cell level, the data were normalized by the median centering method at the proteins level (Supplementary Fig. 1). Then, proteins with expression values in at least 70% of protoplasts were selected for further analysis (Supplementary Table S2). We then imputed all the missing values in the confined dataset using a K nearest neighbors algorithm with $k=3$ as described in the SCP package. Imputed data were then examined for a batch effect. Since the batch effect was appeared to be elevated among TMT sets, we corrected it by utilizing the ComBat function (Leek et al. 2012). As a result, the batch effect was removed as shown in Fig. 3.

To see cellular heterogeneity, we carried out treatment-guided unsupervised hierarchical clustering of protoplasts (Fig. 4A). Overall proteome expression seems to be quite dynamic among protoplasts regardless treatment, indicating cellular heterogeneity in intrinsic proteome expression that may be minimally altered by ABA during the short-term treatment. This result also indicates that it is important to specify cell types before a proper analysis at the single-cell level. Student t test analysis further identified only two upregulated and two downregulated proteins (i.e., greater than 1.23-fold change and better than 0.05 p-value, Fig. 4B and Supplementary Table S2).

To further understand our single-protoplast proteome data, we next performed a bulk proteomic analysis of

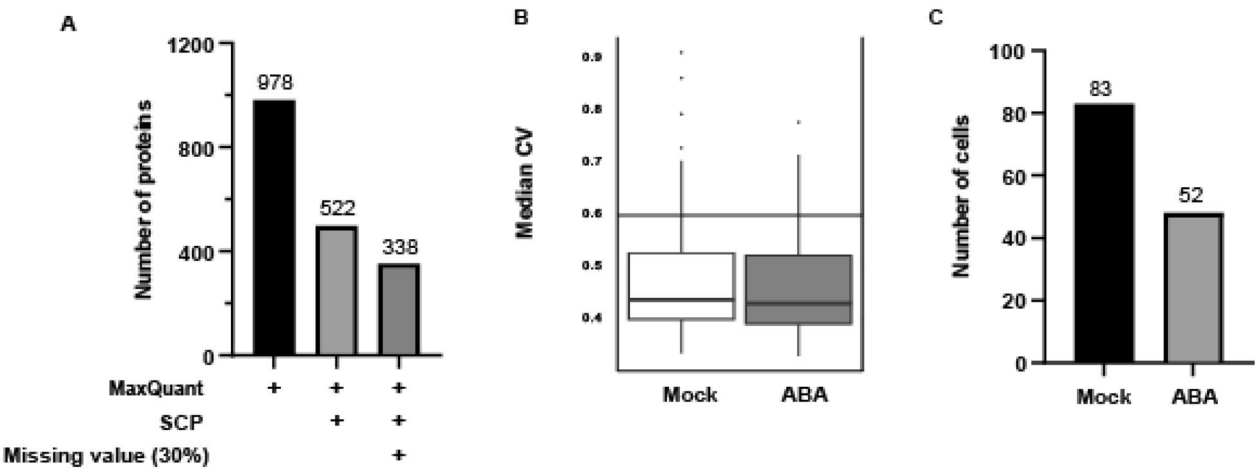

Fig. 2 **A** Number of proteins resulted from each step. **B** Median CV of protoplasts in mock and ABA-treated conditions. **C** Number of protoplasts in mock- and ABA-treated conditions for further data analysis

Table 1 Gene ontology of proteins identified by single-protoplast proteomics

	GO term	Fold enrichment	FDR
GO:BP	glycogen catabolic process (GO:0005980)	28.2	1.52E-02
	arginine biosynthetic process via ornithine (GO:0042450)	28.2	7.29E-04
	carbon fixation (GO:0015977)	26.32	5.08E-18
	reductive pentose-phosphate cycle (GO:0019253)	26.18	1.18E-16
	photosynthesis, dark reaction (GO:0019685)	24.44	7.64E-16
	intracellular nitrogen homeostasis (GO:0141067)	23.5	7.14E-06
	nitrogen utilization (GO:0019740)	23.5	7.11E-06
	ammonia assimilation cycle (GO:0019676)	23.5	7.08E-06
	glycine decarboxylation via glycine cleavage system (GO:0019464)	23.5	7.05E-06
	photosynthetic electron transport in photosystem II (GO:0009772)	22.56	3.11E-09
GO:MF	SHG alpha-glucan phosphorylase activity (GO:0102499)	28.2	2.11E-02
	electron transporter, transferring electrons within the noncyclic electron transport pathway of photosynthesis activity (GO:0045157)	28.2	2.10E-02
	camalexin binding (GO:2,001,147)	28.2	2.09E-02
	chloroplast photosystem II binding (GO:0062068)	28.2	2.08E-02
	intramolecular aminotransferase activity (GO:0016869)	28.2	2.07E-02
	uroporphyrinogen decarboxylase activity (GO:0004853)	28.2	2.06E-02
	triose-phosphate isomerase activity (GO:0004807)	28.2	2.05E-02
	linear malto-oligosaccharide phosphorylase activity (GO:0102250)	28.2	2.04E-02
	electron transporter, transferring electrons from cytochrome b6/f complex of photosystem II activity (GO:0046028)	28.2	2.03E-02
	glutamate synthase (ferredoxin) activity (GO:0016041)	28.2	2.02E-02
GO:CC	TOC-TIC supercomplex I (GO:0061927)	28.2	3.68E-04
	mitochondrial proton-transporting ATP synthase, stator stalk (GO:0000274)	28.2	8.83E-03
	photosystem II antenna complex (GO:0009783)	28.2	8.77E-03
	chloroplast photosystem I (GO:0030093)	28.2	3.65E-04
	proton-transporting ATP synthase, stator stalk (GO:0045265)	28.2	8.71E-03
	photosystem I reaction center (GO:0009538)	25.63	4.15E-13
	endopeptidase Clp complex (GO:0009368)	25.63	4.10E-13
	chloroplastic endopeptidase Clp complex (GO:0009840)	24.67	5.92E-09
	stromule (GO:0010319)	24.58	2.86E-43
	nascent polypeptide-associated complex (GO:0005854)	24.17	1.36E-07

leaves treated with ABA. The detached leaves were incubated with or without 100 μM ABA for 24 h, peptides were prepared for the TMT multiplexing, and pooled peptides were fractionated and analyzed on a high-resolution mass spectrometer (Fig. 5). This bulk proteomic analysis identified a total of 3595 proteins with 83 (~ 2%) upregulated and 187 (~ 5%) downregulated proteins when treated with ABA (Supplementary Table S3). Then we carried out the GO:BP analysis of these altered proteins and resulted in a few important known biological processes and indicated that decreased proteins were largely related to photosynthesis by photosystem I and II. These biological processes also observed in abundant proteins in single-cell data (Fig. 6).

To examine the difference and the similarity between single protoplast and bulk proteomes, we compared a list of proteins identified in single protoplasts with bulk leaf. Of the 338 proteins identified by single-protoplast proteomics, 296 proteins overlapped with the bulk data (Fig. 7A) were used to depict a scatter plot based on their fold changes at the single-cell level and the whole leaf level (Fig. 7B). In addition, we also observed that 44 proteins identified by single-protoplast proteomics were overlapped with differentially expressed proteins in the bulk analysis (Supplementary Figure S2). Although the 44 proteins were known to be involved in biological processes such as photosynthesis and stress response, the difference in quantitation upon ABA treatment between single-protoplast and bulk leaf proteomes raised a question whether this reflected the new biological insights. Among different cell types in a leaf, the majority of isolated protoplast is derived from mesophyll with a higher content of chlorophyll and bigger size (Xu et al. 2021). During

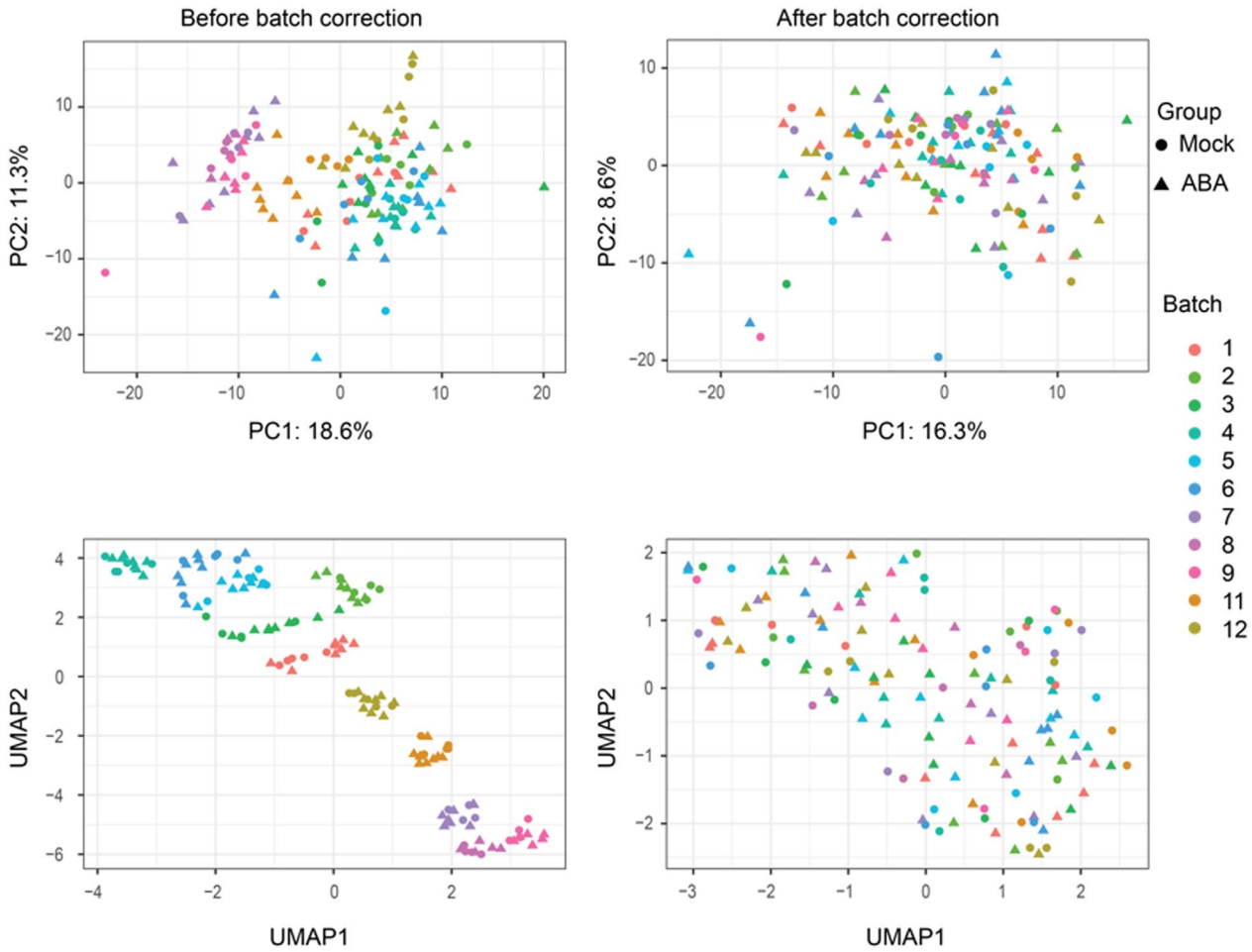

Fig. 3 Principal component analysis (upper panel) and UMAP analysis (lower panel) before and after batch correction

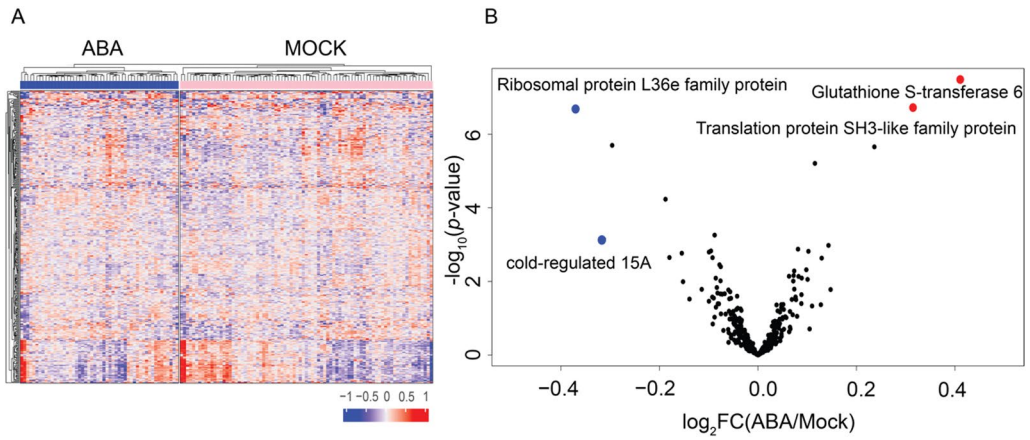

Fig. 4 **A** Unsupervised hierarchical clustering of single protoplasts in each condition. **B** Volcano plot of differentially regulated proteins

dispensing a single protoplast by the CellenONE system, it measured the cell size using the camera system. Thus, we believed that the selected range of cell diameters might be restricted to mesophyll. In addition, a recent study observed that isolating protoplasts led to a stochastic activation of gene expression in

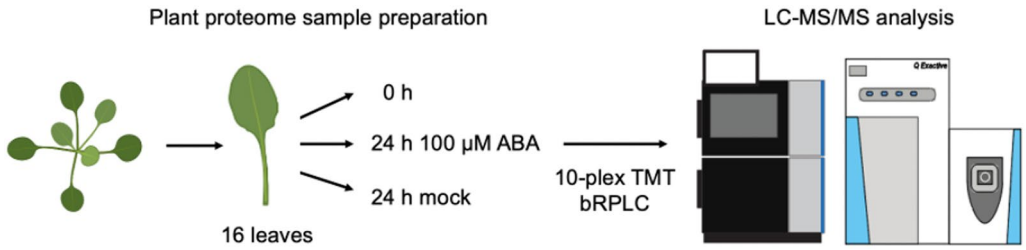

Fig. 5 Experimental workflow of leaf proteomics. A total of nine leaves samples were prepared for a multiplexing experiment (i.e., control, mock, and ABA-treated leaves)

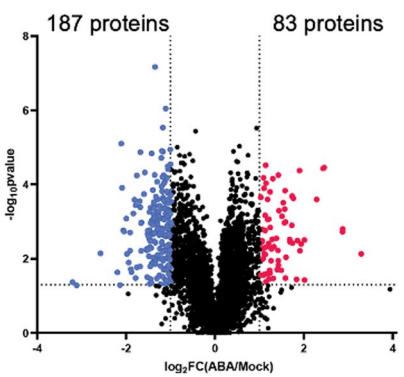

	GO:BP
Increased by ABA	aging (GO:0007568)
	response to osmotic stress (GO:0006970)
	response to stress (GO:0006950)
	response to stimulus (GO:0050896)
Decreased By ABA	photosynthesis, light harvesting in photosystem I (GO:0009768)
	photosynthetic electron transport in photosystem II (GO:0009772)
	photosynthesis, light harvesting in photosystem II (GO:0009769)
	photosynthesis, light harvesting (GO:0009765)

Fig. 6 Volcano plot (left) and GO:BP terms (right) represented by proteins altered by ABA in bulk proteomes of leaves. Many altered proteins were observed with smaller variation

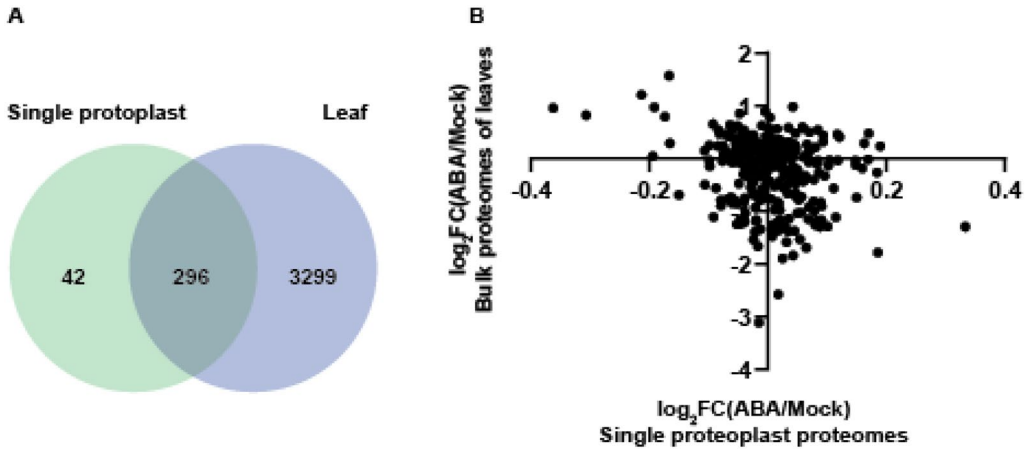

Fig. 7 **A** Comparison of proteins identified in single-cell proteomics analysis and bulk leaf proteomics analysis. **B** Scatter plot of $Log_2FC(ABA/Mock)$ from bulk proteomes of leaves and single-protoplast proteomes

response to stress (Xu et al. 2021). We also observed larger variation in single-protoplast proteomes. Furthermore, proteins that are exclusively identified in single-protoplast proteomics were majorly associated with photosynthetic process and stress response (data not shown). Perhaps, the response to ABA treatment potentially differed between bulk leaf and single cell since protoplast exhibited a different level of cellular stress.

Conclusions

Recent availability in ultra-sensitive high-resolution mass spectrometry and single-cell RNA-seq data strongly appeal researchers in the field of proteomics to develop single-cell proteomics methods. This request promptly made to establish the analyses of single-cell proteomes which may result in novel aspects of cellular processes. Although there have been studies in single-mammalian cell proteomics, there is no attempt to study single-plant cell proteomics. In this study, we explored the possibility of applying the single-cell proteomics technology to a single-protoplast proteomic analysis and identified about a thousand of proteins from single protoplasts. As a result, proteins related to well-known biological processes such as photosynthesis and metabolic processes were identified.

Currently, single-cell proteomics is challenging due to the unmet sensitivity of LC–MS systems and the lack of best practices in sample preparation, resulting in qualitative and quantitative inaccuracy. To overcome this challenge, the utilization of a carrier channel with 200 times more cells was demonstrated to significantly enhance the number of protein identifications. However, it was found that this method significantly affects the quantitative accuracy. Therefore, optimization of the carrier channel is required prior to a single-cell proteomics analysis. Several studies have been conducted to find an optimal number of cells in a carrier channel using different mass spectrometers. For example, the optimal number of cells as a carrier in an Orbitrap Eclipse mass spectrometer is about 20 times, whereas it is 200-fold on a Q-Exactive mass spectrometer (Cheung et al. 2021; Ctortecka et al. 2021; Specht and Slavov 2020). In addition, for data normalization among each TMT set, the same amount of proteins equivalent to 5 cells should be used for the reference channel, unlike using cells from different populations for carriers and reference at the same times as in this study. As the result of the benchmarking study, the SCoPE2 workflow was further developed with the new 200 times more cells as a carrier for signal boosting and 5 times more cells as a reference for normalization. This method has now improved the single-cell proteomics qualitatively and quantitatively. Nonetheless, several intrinsic factors such as unavoidable isotopic impurities of isobaric reagents and co-isolation and co-fragmentation of precursors affect quantitative accuracy when utilizing MS2-based quantitation (Specht et al. 2021; Searle and Yergey 2020). In addition, an analysis of datasets produced by single-cell proteomics is still a hurdle. Up to date, there is no best practice for a single-cell proteomics data analysis where the batch effect and missing values from different sets of samples should be properly handled for downstream data analysis.

In conclusion, we have successfully analyzed single-plant cell proteomes. We believe that this study will contribute valuable insights into the field of single-plant cell proteomics in the near future.

Abbreviations

SCP	Single-cell proteomics
DAE	Days after an emergency
ABA	Abscisic acid
MES	2-(N-morpholino) ethanesulfonic acid
DDM	Dodecyl-beta-D-maltopyranoside
TEAB	Triethylammonium bicarbonate
LC	Liquid chromatography
MS	Mass spectrometry
FA	Formic acid
ACN	Acetonitrile
AGC	Automatic gain control
TMT	Tandem mass tag
GO	Gene ontology
BP	Biological process
MF	Molecular function
CC	Cellular component

Supplementary Information

The online version contains supplementary material available at https://doi.org/10.1186/s40543-024-00457-x.

Supplementary material 1: Supplementary Figure S1. Box plots of log2 protein intensity for each cell after normalization.

Supplementary material 2: Supplementary Figure S2. Comparison of proteins identified in single cell proteomics analysis and differentially expressed protein in bulk leaf proteomics analysis

Supplementary material 3.

Supplementary material 4.

Supplementary material 5.

Supplementary material 6.

Acknowledgements

We thank the members of the QBIO laboratory for their help.
Author contributions
M-SK, POL, and JYK conceived the study. JYL performed LC-MS. HMV, FI, JHL, and MJ prepared proteome samples, YK, SP, JL, and HRW prepared plant samples. M-SK, POL, JYK, JYL, HMV, JHL, and HRW wrote the manuscript.

Author contributions

M-SK, POL, and JYK conceived the study. JYL performed LC-MS. HMV, FI, JHL, and MJ prepared proteome samples, YK, SP, JL, and HRW prepared plant samples. M-SK, POL, JYK, JYL, HMV, JHL, and HRW wrote the manuscript.

Funding

This research was supported by the National Research Foundation of Korea (NRF) grants (2019R1A2C1089459 to P.O.L.; 2022R1A2C2013377 to M.-S.K.; DGIST R&D program [24-CoE-BT-01] to M.-S.K.) and by Research Program (2022M3H9A2096186 to J.Y.K.) of the National Research Foundation (NRF) funded by the Korean government (MSIT).

Availability of data and materials

All data analyzed during this study are included in this published article as Supplementary Tables 1–3. Raw data and search results were deposited to ProteomeXchange Consortium (Deutsch et al. 2023) via PRIDE (Perez-Riverol et al. 2022) under project accession ID PXD052208.

Declarations

Competing interests
The authors declare no conflict of interest.

Received: 21 December 2023 Accepted: 19 July 2024
Published online: 31 July 2024

References

Budnik B, Levy E, Harmange G, Slavov N. Scope-ms: mass spectrometry of single mammalian cells quantifies proteome heterogeneity during cell differentiation. Genome Biol. 2018;19:1–12.
Cheung TK, Lee C-Y, Bayer FP, McCoy A, Kuster B, Rose CM. Defining the carrier proteome limit for single-cell proteomics. Nat Methods. 2021;18(1):76–83.
Clark NM, Elmore JM, Walley JW. To the proteome and beyond: advances in single-cell omics profiling for plant systems. Plant Physiol. 2022;188(2):726–37.
Ctortecka C, Stejskal K, Krssakova G, Mendjan S, Mechtler K. Quantitative accuracy and precision in multiplexed single-cell proteomics. Anal Chem. 2021;94(5):2434–43.
Ctortecka C, Hartlmayr D, Seth A, Mendjan S, Tourniaire G, Udeshi ND, Carr SA, Mechtler K. An automated nanowell-array workflow for quantitative multiplexed single-cell proteomics sample preparation at high sensitivity. Mol Cell Proteomics. 2023;22(12):100665.
Deutsch EW, Bandeira N, Perez-Riverol Y, Sharma V, Carver JJ, Mendoza L, Kundu DJ, Wang S, Bandla C, Kamatchinathan S, et al. The proteomexchange consortium at 10 years: 2023 update. Nucleic Acids Res. 2023;51(D1):D1539–48.
Keller BO, Sui J, Young AB, Whittal RM. Interferences and contaminants encountered in modern mass spectrometry. Anal Chim Acta. 2008;627(1):71–81.
Kovtun Y, Chiu W-L, Tena G, Sheen J. Functional analysis of oxidative stress-activated mitogen-activated protein kinase cascade in plants. Proc Natl Acad Sci. 2000;97(6):2940–5.
Lee S, Vu HM, Lee J-H, Lim H, Kim M-S. Advances in mass spectrometry-based single cell analysis. Biology. 2023;12(3):395.
Leek JT, Johnson WE, Parker HS, Jaffe AE, Storey JD. The sva package for removing batch effects and other unwanted variation in high-throughput experiments. Bioinformatics. 2012;28(6):882–3.
Liang Y, Acor H, McCown MA, Nwosu AJ, Boekweg H, Axtell NB, Truong T, Cong Y, Payne SH, Kelly RT. Fully automated sample processing and analysis workflow for low-input proteome profiling. Anal Chem. 2020;93(3):1658–66.
Mi H, Muruganujan A, Thomas PD. Panther in 2013: modeling the evolution of gene function, and other gene attributes, in the context of phylogenetic trees. Nucleic Acids Res. 2012;41(D1):D377–86.
Montes C, Zhang J, Nolan TM, and Walley JW. Single-cell proteomics differentiates arabidopsis root cell types. *bioRxiv*, pages 2024;2024–04.
Perez-Riverol Y, Bai J, Bandla C, Garćıa-Seisdedos D, Hewapathirana S, Kamatchinathan S, Kundu DJ, Prakash A, FrericksZipper A, Eisenacher M, et al. The pride database resources in 2022: a hub for mass spectrometry-based proteomics evidences. Nucleic Acids Res. 2022;50(D1):D543–52.
Searle BC, Yergey AL. An efficient solution for resolving itraq and tmt channel cross-talk. J Mass Spectrom. 2020;55(8):e4354.
Specht H, Slavov N. Optimizing accuracy and depth of protein quantification in experiments using isobaric carriers. J Proteome Res. 2020;20(1):880–7.
Specht H, Emmott E, Petelski AA, Huffman RG, Perlman DH, Serra M, Kharchenko P, Koller A, Slavov N. Single-cell proteomic and transcriptomic analysis of macrophage heterogeneity using scope2. Genome Biol. 2021;22:1–27.
Thomas PD, Ebert D, Muruganujan A, Mushayahama T, Albou L, Mi H. Panther: making genome-scale phylogenetics accessible to all. Protein Sci. 2022;31(1):8–22.
Vanderaa C, Gatto L. Replication of single-cell proteomics data reveals important computational challenges. Expert Rev Proteomics. 2021;18(10):835–43.
Vanderaa C, Gatto L. Revisiting the thorny issue of missing values in single-cell proteomics. J Proteome Res. 2023;22(9):2775–84.
Woo HR, Kim HJ, Lim PO, Nam HG. Leaf senescence: systems and dynamics aspects. Annu Rev Plant Biol. 2019;70:347–76.
Xu M, Du Q, Tian C, Wang Y, Jiao Y. Stochastic gene expression drives mesophyll protoplast regeneration. Sci Adv. 2021;7(33):eabg8466.
Zhu Y, Piehowski PD, Zhao R, Chen J, Shen Y, Moore RJ, Shukla AK, Petyuk VA, Campbell-Thompson M, Mathews CE, et al. Nanodroplet processing platform for deep and quantitative proteome profiling of 10–100 mammalian cells. Nat Commun. 2018;9(1):882.

Publisher's Note